Nonequilibrium positive column

J. H. Ingold
One Bratenahl Place, Suite 610, Cleveland, Ohio 44108
(Received 19 May 1997)

The dc positive column is modeled with a system of balance equations based on moments of the radially dependent Boltzmann equation taken after the two-term Legendre expansion of the electron energy distribution function is made. The importance of the electron energy balance equation, which is frequently ignored in positive column analysis, is emphasized. A key assumption is that electron transport coefficients and collision frequencies in the nonequilibrium regime have the same relation to the average energy as in the equilibrium regime, according to a zero-dimensional Boltzmann solution for a particular value of average energy. Because of this assumption, the model makes a smooth transition to the traditional equilibrium model with radially constant average energy at sufficiently high pressure. Model results in the nonequilibrium regime agree closely with published results of a numerical solution of the one-dimensional Boltzmann equation, including results for radial heat flow in the electron gas with radially varying average energy. It is shown that three separate processes account for radial heat flow: convection, conduction, and diffusion. In the example chosen for illustration of the method, the convection component is small, while the conduction and diffusion components are large and opposite in direction, nearly canceling each other. [S1063-651X(97)00311-5]

PACS number(s): 51.50.+v, 52.25.Fi, 52.80.−s

I. INTRODUCTION

A. General remarks

The consensus throughout the period 1920–1970 appears to be that the electron energy distribution function (EEDF) in the dc positive column is Maxwellian and that the average energy of the electrons is radially invariant. This consensus is supported in review articles by Druyvesteyn and Penning [1] and Francis [2] in which positive column pedagogy is based on Maxwellian EEDF's, although the possibility of non-Maxwellian EEDF's at *low current* is recognized in both review articles. Direct consequences of the Maxwellian EEDF assumption are that (i) the average energy, transport coefficients, and collision frequencies are radially invariant; (ii) the power input per unit volume due to Joule heating and the power dissipated per unit volume due to elastic and inelastic collisions are equal in each volume element of the positive column; and (iii) radial effects such as heat flow are negligible. A positive column having these characteristics is said to be operating in the *local regime* because electron properties are in equilibrium with the axial electric field in each volume element. But what about other EEDF forms? If transport coefficients and collision frequencies are radially invariant, then they can be parametrized by the axial electric field as in a zero-dimensional (0D) Boltzmann calculation, leading to an improvement over the Maxwellian EEDF assumption. Strictly speaking, when electron-electron collisions can be ignored, then a Maxwellian EEDF results only when the electron-atom momentum-transfer collision frequency is independent of electron energy. Realizing that real gases do not have this kind of collision frequency, Blank [3] asks under what conditions can it be assumed that positive column transport coefficients and collision frequencies are radially invariant, similar to conditions found in a drift tube experiment. In agreement with Bernstein and Holstein [4], Blank concludes that this assumption is valid for an energy-dependent momentum-transfer collision frequency when ''the electron energy relaxation length is small compared with the macroscopic length scale, ...'' To put this conclusion in perspective, consider a neonlike gas with an atomic mass of 20 amu and electron-atom momentum-transfer cross section Q_{ea} of 2.6 Å^2. Blank's condition expressed in mathematical form is $PR \gg 0.283\sqrt{M/m}Q_{ea}^{-1} = 21$ Torr cm, where P is the gas pressure in Torr, R is the positive column radius in cm, M/m is the mass ratio of atoms and electrons, and Q_{ea} is expressed in Å^2. It is shown later in the present article that the value of PR must be in the range 50–100 Torr cm for the assumption of radially invariant transport coefficients and collision frequencies in a neon positive column to be valid.

Evidently, when $PR < 0.283\sqrt{M/m}Q_{ea}^{-1}$, the local model is not valid. It is argued in [4] that radial effects become important at low pressure, causing electron properties such as average energy and axial drift velocity to have significant radial variation. In this case, transport coefficients and collision frequencies cannot be parametrized by the axial electric field as in a 0D Boltzmann calculation because the axial electric field is independent of radial position. A positive column having these characteristics is said to be operating in the *nonlocal regime*. Radial terms must be taken into account in solving the Boltzmann equation, meaning that a 1D Boltzmann solution is required in the nonlocal regime. Incidentally, the words *local* and *equilibrium* are used interchangeably in the present article, as are the words *nonlocal* and *nonequilibrium*.

In an important series of papers beginning in 1974, Tsendin [5] extended the positive column work begun by Bernstein and Holstein and elucidated further by Blank. Tsendin and followers cite several features of the nonlocal model that are different from those of the local model: (i) The Boltzmann relation between the electron density $n(r)$, space-charge potential $\phi(r)$, and electron temperature θ no longer holds, i.e., $n(r) \neq n(0)\exp[\phi(r)/\theta]$; (ii) there is a significant

radial variation in the average energy of electrons, hence in transport coefficients and collision frequencies; (iii) likewise, there can be a significant difference between the power input by Joule heating and the power dissipation due to collisions in a given volume element of the discharge; (iv) to account for (iii), a significant amount of heat must flow inward in the electron gas; and (v) the wall potential relative to axis value is much less. These differences are corroborated by recently published numerical solutions of the 1D Boltzmann equation [6]. Therefore, it appears that the traditional local model is inadequate at PR values on the order of 10 and smaller.

The purpose of this article is to show that traditional local theory of the dc positive column can be extended to the nonlocal regime. In Sec. II the traditional local moment model with radially invariant average energy is extended to the nonlocal regime by including the electron energy balance equation, which accounts for radially varying average energy, achieving very good qualitative agreement with Ref. [6]. The extended formulation is based on moments of the 1D Boltzmann equation taken after the two-term Legendre expansion is made. In Sec. III the boundary between local and nonlocal regimes is established by starting with the traditional model extended as described above, then assuming that average energy is radially invariant, and then deriving a relationship that must be satisfied if this assumption is to be valid. In this way, a pressure boundary between local and nonlocal behavior is defined.

B. Brief review of 1D Boltzmann methods

Before turning to the subject of the present article, the nonlocal moment method, it is instructive to review 1D Boltzmann methods in use today for analyzing the dc positive column. Methods that do not start with the 1D Boltzmann equation and the two-term Legendre expansion will not be discussed. Those that do can be divided arbitrarily into four categories: (i) nonlocal kinetic method, valid at all PR; (ii) nonlocal kinetic approximation method, valid at low PR; (iii) local moment method, valid at high PR, but often used at low PR; and (iv) nonlocal moment method, valid at all PR. The first three methods are described briefly below in this section; the fourth is discussed in detail in Sec. II.

1. Nonlocal kinetic method

The nonlocal kinetic method is a first-principles method that is valid at all values of PR for which the 1D Boltzmann equation based on the two-term Legendre expansion of the EEDF is valid. The EEDF is denoted by $f(\mathbf{r},\mathbf{v})$ and the two-term expansion is

$$f(\mathbf{r},\mathbf{v}) = f_0(r,v) + v^{-1}\mathbf{v}\cdot\mathbf{f}_1(r,v).$$

Measurable properties of the positive column are calculated directly from f_0 and f_1.

A prime example of this method was published recently by Uhrlandt and Winkler [6]. In this reference, the 1D Boltzmann equation is solved numerically after the two-term Legendre expansion is made. The radial space-charge potential distribution and axial field taken from measurements in a neon positive column with $PR = 1.3$ Torr cm and current $I = 10$ mA are assumed in the calculation. In other words, Poisson's equation and the ion momentum balance equation are not solved simultaneously with the 1D Boltzmann equation. Uhrlandt and Winkler find that all electron properties vary with radial position and on axis there is a large difference between Joule heat input per unit volume and collision loss per unit volume. Results of the nonlocal moment method described in the present paper are compared with results of Uhrlandt and Winkler in Sec. II, with very good qualitative agreement.

Finding solutions at several different values of PR, Busch and Kortshagen [7] find a radial variation in the electron properties similar to that found by Uhrlandt and Winkler for values of PR on the order of unity. For $PR = 28$ Torr cm and above, however, Busch and Kortshagen find that the average electron energy is radially invariant except very near the wall of the positive column, which suggests that the positive column operates in the local regime at this and higher values of PR. It is shown in Sec. III of this article that the nonlocal moment method makes a smooth transition to the local moment method at sufficiently high values of PR, thus establishing the boundary between them.

The advantage of the nonlocal kinetic method is accurate calculation of the important physical processes taking place in the positive column. A disadvantage is its complexity, which makes it computationally intensive, especially when Poisson's equation and electron-electron collisions are taken into account. Perhaps it is for this reason that the method is just now coming into use.

2. Nonlocal kinetic approximation method

The nonlocal kinetic approximation method [4,5] is also based on the two-term Legendre expansion of the EEDF. However, the solution of the 1D Boltzmann equation for f_0 and $\mathbf{f}_1$ is avoided by assuming further that f_0 and $\mathbf{f}_1$ can be expanded according to the scheme

$$f_0(r,\epsilon) = f_{00}(\epsilon) + f_{01}(r,\epsilon) + \cdots ,$$

$$\mathbf{f}_1(r,\epsilon) = \mathbf{f}_{10}(r,\epsilon) + \mathbf{f}_{11}(r,\epsilon) + \cdots ,$$

where the total energy $\epsilon = \frac{1}{2}mv^2 - e\phi(r)$ and f_{00} is given by the 0D Boltzmann equation obtained from the 1D Boltzmann equation by radially averaging each term, while the radial component of $\mathbf{f}_{10}(r,\epsilon)$ is taken to be zero. The results are similar to those of the first-principles method at low values of PR, but start diverging near $PR = 1$. An advantage of this model is that it is not as computationally intensive as the first-principles method. A disadvantage is that its validity is restricted to small values of PR.

3. Local moment method

The local moment method includes the classical ambipolar diffusion theory of Schottky [8] and the free-fall theory of Tonks and Langmuir [9]. This method is based not on the solution of the 1D Boltzmann equation, but on moments of it, moments of either the pristine 1D Boltzmann equation or the equations for f_0 and $\mathbf{f}_1$. A key assumption of this method is that electrons are in *equilibrium* with the axial electric field, implying that the energy imparted to the electrons by a steady, uniform field is exactly balanced by energy lost in elastic and inelastic collisions with heavy particles *in each*

TABLE I. Comparison of the local moment method with other methods. $\overline{n}=(2/R^2)\int n(r)r\,dr$; $\overline{\nu_i}=(2/R^2)\int n(r)\nu_i(r)r\,dr/\overline{n}$; $-\phi_w$ is the wall potential relative to the axis value.

Gas type	Method	E_z (V/cm)	ϕ_w (V)	$n(0)$ (10^{10} cm^{-3})	$\overline{\nu_i}$ (10^5 sec^{-1})	P[a]	Ref.
Helium	Nonlocal[b]						
$PR=0.045$ Torr cm	MC						
$I=10$ mA	CS	48	52	6.0	450	Yes	[14]
$R=1$ mm	Local 0D[c]	39	84	11	400	Yes	[13]
	Local max[d]	41	81	11	400	Yes	[13]
Argon	Nonlocal	12	15			No	[16]
$PR=0.85$ Torr cm	MC	12	18			No	[15]
$\overline{n}=1\times10^{10}$ cm^{-3}	CS	11	17	2.6	1.1	No	[17]
$R=1$ cm	Local 0D	15	52	2.5	2.2	Yes	[13]
	Local max	1.5	13	2.5	0.55	Yes	[13]
Argon	Nonlocal	6	16			No	[16]
$PR=0.28$ Torr cm	MC	6	17			No	[15]
$\overline{n}=1\times10^{10}$ cm^{-3}	CS	6.3	17	2.2	3	No	[17]
$R=1$ cm	Local 0D	7.4	53	2.3	3.5	Yes	[13]
Argon	Nonlocal	1.4	24			No	[16]
$PR=0.0085$ Torr cm	MC	1.4	24			No	[15]
$\overline{n}=1\times10^{10}$ cm^{-3}	CS	1.4	24		6.7	No	[17]
$R=1$ cm	Local 0D	0.9	64	2.1	5.1	Yes	[13]
	Local max	0.5	29	1.9	3.2	Yes	[13]
Neon	Nonlocal	2.7	41			No	[5]
$PR=0.1$ Torr cm	MC						
$I=10$ mA	CS						
$R=1$ cm	Local 0D	2.5	59	0.33	7.9	Yes	[13]

[a]Yes in this column means that Poisson's equation is solved self-consistently with equations of motion, etc., to give the radial potential distribution. No means that either the radial potential distribution is assumed or the plasma (ambipolar) approximation $n(r)=n_i(r)$ is assumed.

[b]Nonlocal means the nonlocal kinetic approximation method.

[c]Local 0D means the local moment method with 0D Boltzmann EEDF.

[d]Local max means the local moment method with Maxwellian EEDF.

volume element of the discharge. In mathematical terms, *equilibrium* implies that spatial and temporal derivatives of the EEDF can be ignored when solving the Boltzmann equation. The steady, uniform motion of electrons under these conditions is accurately described by transport coefficients and collision frequencies, which, by custom, are parametrized by E_z/N, the ratio of the axial electric field to the gas density [10].

Most theoretical treatments of the positive column today can be classified in this category. Furthermore, this is the method universally chosen for pedagogical purposes in review articles and books on the positive column. The first two moments are used in conjunction with ion momentum balance and Poisson's equation to form a complete set of equations to be solved for the radial variation of the electron density, ion density, radial current density, and radial electric field. The average electron energy is radially invariant by assumption. The third moment is used solely to deduce the value of the axial electric field needed to make the power input (Joule heat) per unit volume equal to the power output (collision loss) per unit volume. The advantage of this model is its computational simplicity in comparison with the two models discussed above.

One disadvantage is the loss of accuracy due to the necessity of guessing the form of the EEDF used to evaluate the moments. In other words, the EEDF must be assumed to evaluate transport coefficients and collision frequencies appearing in individual terms in the moment equations. Examples are the (i) one-temperature Maxwellian EEDF [8,9], (ii) two-temperature Maxwellian EEDF [11] (iii) Lyaguschenko EEDF [12], and (iv) 0D Boltzmann EEDF [13]. Computer codes for some applications have switches that enable any of the above at the whim of the computer analyst.

There is further loss of accuracy when this model is applied to cases with small values of PR. This happenstance may be due in part to the difficulty encountered when one tries to establish the PR range of validity of this method. As Tsendin [5] points out, this method is valid at small PR only when the EEDF is Maxwellian. When the EEDF is other than Maxwellian, then it should not be used for values of PR smaller than 30, as suggested in Ref. [7]. Table I shows what happens when this admonition is ignored. This table shows a comparison of measurable quantities for the He, Ar, and Ne positive columns calculated by several different theoretical methods, including Monte Carlo (MC) [15] and convective

scheme (CS) [14,17] methods, which do not start with the 1D Boltzmann equation. In every case, the wall potential found by the local moment method with a 0D EEDF is significantly higher than wall potential found by other means, a result that can be attributed directly to the assumption of radially constant average energy. Curiously, the local moment method with a Maxwellian EEDF gives a wall potential closer to that of MC and CS methods, even though the average energy is radially invariant. The low wall potential in this case is due to the low value of average energy needed to provide sufficient ionization when the EEDF is Maxwellian. In addition to a low average energy, the axial field is too low for the argon examples with the Maxwellian EEDF listed in Table I.

In view of these inaccuracies, it must be concluded that the local moment method is inadequate for describing the positive column behavior at low PR. It is shown in the next section that these shortcomings are absent from the nonlocal moment method obtained by adding electron energy balance with radially varying average energy to the local moment method.

II. NONLOCAL MOMENT METHOD

A. General remarks

This section deals with an extension of the local moment method, or local model, of the dc positive column to the nonlocal regime where electrons are no longer in equilibrium with the axial field. The extension is accomplished by including the energy balance equation obtained by taking the third moment of the 1D Boltzmann equation after the two-term Legendre expansion is made. As with the local moment method, the EEDF must be assumed in order to evaluate transport coefficients and collision frequencies appearing in the moment equations. A key assumption of the nonlocal moment method is that transport coefficients and collision frequencies bear the same relation to the average energy, which is a function of the radial position in the nonequilibrium positive column, as they do in the local moment model, according to a 0D Boltzmann solution. This assumption is tantamount to assuming a form for the EEDF that depends on the electron density, average velocity, and average energy in a particular way that ensures correct values of transport quantities when electrons are in equilibrium with the electric field [18]. This method differs from the local moment method in that the average energy, transport coefficients, and collision frequencies can vary across the positive column, even though the axial field does not. This method has several advantages over the local moment method, not the least of which is validity over the entire range of PR, just as with the first-principles nonlocal kinetic method. Because the nonlocal moment method makes a transition naturally to the local moment method at high values of PR, it is straightforward to establish the PR range of validity of the local moment method. This is done in Sec. III.

B. Equations

Formulation of this problem is based on moments of the Boltzmann equation taken after the two-term Legendre expansion is made. This procedure leads to the following equations for the dc positive column with the electron gas characterized by particle density n, particle current density $\mathbf{\Gamma}$, average energy u, and heat current density $\mathbf{H}$:

$$\mathbf{\Gamma} = -\nabla(nD) - \mu \mathbf{E} n, \tag{1}$$

$$\nabla \cdot \mathbf{\Gamma} = \nu_i n, \tag{2}$$

$$\mathbf{H} = -\nabla(nG) - \beta \mathbf{E} n, \tag{3}$$

$$\nabla \cdot \mathbf{H} = -\mathbf{\Gamma} \cdot \mathbf{E} - \left(2 \frac{m}{M} \nu_u u + \nu_x V_x + \nu_i V_i \right) n, \tag{4}$$

where D, μ, G, and β are transport coefficients defined by Allis [9], ν_u is elastic energy exchange collision frequency, $\nu_{x,i}$ is excitation or ionization frequency, and $V_{x,i}$ is the excitation or ionization energy. D and μ are the well-known coefficients of particle diffusion and mobility, respectively, while Allis [19] calls G and β the coefficients of heat diffusion and thermoelectricity, respectively. The electric field $\mathbf{E}$ has two components: the imposed axial field E_z, which is independent of r and z, and the radial space charge field $E_r(r)$. The vectors $\mathbf{\Gamma}$ and $\mathbf{H}$ each have axial and radial components that vary with radial position.

Ions with zero temperature, mobility μ_i, mass m_i, and density n_i are characterized by the ion momentum balance

$$\Gamma_r = -\frac{\mu_i}{r} \frac{d}{dr} \left[r \left(\frac{m_i \Gamma_r^2}{e n_i} \right) \right] + \mu_i E_r n_i, \tag{5}$$

where it is assumed that $\Gamma_{ir} = \Gamma_r$, reflecting the assumption of a steady state. Finally, Poisson's equation relating the radial space-charge field to the space-charge density is

$$\frac{1}{r} \frac{d(rE_r)}{dr} = \frac{e}{\epsilon} (n_i - n), \tag{6}$$

where $e = 1.6 \times 10^{-19}$ C is the electronic charge and $\epsilon = 8.85 \times 10^{-14}$ C/V/cm is the permittivity.

Equations (1), (2), (5), and (6) form the basis of the local model with radially invariant average energy, transport coefficients, etc. Extension of the local model to the nonlocal regime is accomplished by the addition of Eqs. (3) and (4) to account for the radial heat flow in the electron gas with radially varying average energy.

The objective of this section is to apply the equations given above to the neon positive column investigated by Uhrlandt and Winkler [6], who applied the nonlocal kinetic method to a 0.75-Torr neon discharge in a tube of 1.7 cm radius with a current of 10 mA. They showed that such a discharge operates in the nonlocal regime because the power expended in collisions is not equal to the power generated by the external field in each volume element of the discharge. On axis, for example, they found that Joule heating amounts to 6.4 mW/cm^3, while the power expended in collisions amounts to 16 mW/cm^3. To maintain this discharge in the steady state, a significant amount of energy flow from the outer region of the discharge to the inner region is required.

To reach this objective, the approach taken here is to assume a form for the EEDF that depends on the electron density, average velocity, and average energy in a particular way

that ensures correct values of transport quantities when electrons are in equilibrium with the electric field. In other words, transport coefficients are assumed to be functions of the radially varying average energy, not of the radially constant E_z/N. Still another way of saying this is to say that transport coefficients are parametrized by the average energy, not by E_z/N [20]. The parametrization is carried out by solving the 0D Boltzmann equation and constructing a table of transport coefficients and collision frequencies versus the average energy and then solving Eqs. (1)–(6) for the radial variation of the six quantities $n(r)$, $n_i(r)$, $u(r)$, $\Gamma_r(r)$, $H_r(r)$, and $E_r(r)$.

To solve Eqs. (1)–(6) by a Runge-Kutta technique, it is convenient to eliminate **E** from Eq. (3) by means of Eq. (1) to give

$$\mathbf{H}=\frac{\beta}{\mu}\,\Gamma+\frac{\beta}{\mu}\,\boldsymbol{\nabla}(nD)-\boldsymbol{\nabla}(nG),$$

so that

$$H_r=\frac{\beta}{\mu}\,\Gamma_r+\left(\frac{\beta}{\mu}-\frac{G}{D}\right)D\,\frac{dn}{dr}-n\left(\frac{\partial G}{\partial u}-\frac{\beta}{\mu}\,\frac{\partial D}{\partial u}\right)\frac{du}{dr}. \quad (7)$$

The first term on the right-hand side represents an energy flow due to convection. The second term on the right-hand-side represents an energy flow due to diffusion, which can be directed either inward or outward, depending on the relative magnitudes of β/μ and G/D. When the EEDF is Maxwellian, due to electron-electron collisions, for example, then $\beta/\mu-G/D=0$, resulting in little or no energy flow due to diffusion or conduction. However, in the case of neon when electron-electron collisions are ignored, it will be seen that the quantity $\beta/\mu-G/D$ is positive, so that the energy flow due to diffusion is directed inward, accounting for the apparent nonlocal behavior of the low-current neon discharge [21]. The third term on the right-hand side represents energy flow due to thermal conduction. The quantity

$$n\left(\frac{\partial G}{\partial u}-\frac{\beta}{\mu}\,\frac{\partial D}{\partial u}\right)$$

is nothing but the thermal conductivity of the electron gas; this quantity is positive so that energy flow due to thermal conduction is directed outward in the neon discharge.

The energy balance equation (4) becomes

$$\frac{1}{r}\,\frac{d(rH_r)}{dr}=\mu nE_z^2-\Gamma_rE_r-\left(2\,\frac{m}{M}\,\nu_u u+\nu_xV_x+\nu_iV_i\right)n, \quad (8)$$

when the relation $\Gamma_z=-\mu nE_z$ is used to eliminate Γ_z. The second term on the right-hand side of this equation represents a cooling effect due to the radial electron current density flowing against the radial space-charge field. This term is neglected in the present treatment because it generally is small compared with the term μnE_z^2. Γ_r lies between $\mu_in_iE_r$ and $n_i\sqrt{-2e\phi/m_i}$, where the space-charge potential $\phi(r)$ is related to E_r by

$$\phi(r)=-\int_0^r E_r(\rho)\,d\rho,$$

depending on whether the ion motion is limited by ion mobility or by ion inertia. In the mobility-limited case, for example, $\Gamma_rE_r=\mu_in_iE_r^2$, which is small compared with μnE_z^2, except, perhaps, very near the wall.

For clarity, the equation system is repeated here. There are six equations to be solved for the six quantities $n(r)$, $u(r)$, $n_i(r)$, $\Gamma_r(r)$, $H_r(r)$, and $E_r(r)$. The six equations are

$$\frac{dn}{dr}=\left[D\,\frac{\partial}{\partial u}\left(\frac{G}{D}\right)\right]^{-1}\left[-\frac{1}{D}\,\frac{\partial G}{\partial u}\,\Gamma_r+\frac{1}{D}\,\frac{\partial D}{\partial u}\,H_r+\left(\frac{\beta}{\mu}\,\frac{\partial D}{\partial u}-\frac{\partial G}{\partial u}\right)\frac{\mu}{D}\,nE_r\right], \quad (9)$$

$$\frac{du}{dr}=\left[D\,\frac{\partial}{\partial u}\left(\frac{G}{D}\right)\right]^{-1}\left[\frac{G}{D}\,\frac{\Gamma_r}{n}-\frac{H_r}{n}-\left(\frac{\beta}{\mu}-\frac{G}{D}\right)\mu E_r\right], \quad (10)$$

$$\frac{dn_i}{dr}=\left(\frac{m_i\Gamma_r^2}{en_i^2}\right)^{-1}\left[\Gamma_r\left(\frac{1}{\mu_i}+\frac{2m_i\nu_i}{e}\,\frac{n}{n_i}\right)-\frac{1}{r}\,\frac{m_i\Gamma_r^2}{en_i}-n_iE_r\right], \quad (11)$$

$$\frac{1}{r}\,\frac{d(r\Gamma_r)}{dr}=\nu_in, \quad (12)$$

$$\frac{1}{r}\,\frac{d(rH_r)}{dr}=\mu nE_z^2-\left(2\,\frac{m}{M}\,\nu_u u+\nu_xV_x+\nu_iV_i\right)n, \quad (13)$$

$$\frac{1}{r}\,\frac{d(rE_r)}{dr}=\frac{e}{\epsilon}\,(n_i-n). \quad (14)$$

C. Boundary conditions

Six boundary conditions are needed to specify a unique solution to this set of six first-order equations. By symmetry,

$$\Gamma_r(0)=0,\quad H_r(0)=0,\quad E_r(0)=0. \quad (15)$$

These conditions ensure that radial gradients $n'(0)=u'(0)=0$. However, because the right-hand side of Eq. (11) appears to have a singularity at $r=0$, conditions (15) alone do not ensure that $n_i'(0)=0$. It is necessary to apply l'Hôpital's rule to the right-hand side of Eq. (11) and impose the condition that the numerator of the resulting quantity be zero at $r=0$ to ensure a zero ion density gradient on axis [22]. Following this procedure gives

$$\frac{\nu_{i0}}{\mu_i}\,n_0\left(1+\frac{3}{2}\,\frac{\nu_{i0}}{\nu_{im}}\,\frac{n_0}{n_{i0}}\right)-\frac{e}{\epsilon}\,(n_{i0}-n_0)n_{i0}=0, \quad (16)$$

where subscript 0 means evaluated at $r=0$ and $\nu_{im}=e/m_i\mu_i$ is the ion-neutral momentum-transfer collision frequency.

The remaining two boundary conditions are conditions on Γ_r and H_r that must be satisfied at the wall located at $r=R$, where R is the discharge tube radius. These two conditions follow from the assumption that the wall emits neither electrons nor electron energy back into the discharge. The

two conditions are derived from the Legendre expansion for the EEDF as follows. The total current of electrons going in the $-r$ direction at the wall is

$$\Gamma_-(R)=2\pi\int_0^{-1}\int_0^{\infty}\mu v\ f(R,\mu,v)v^2dv\ d\mu, \qquad (17)$$

where μ is not the electron mobility, but the cosine of the angle between **v** and the direction perpendicular to the wall. If no electrons are emitted by the wall, then the total particle current directed inward at the wall must be zero. This condition is expressed mathematically by the equation

$$\Gamma_-(R)=2\pi\int_0^{-1}\int_0^{\infty}\mu v[f_0(R,v)+\mu f_{1r}(R,v)]v^2dv\ d\mu = 0. \qquad (18)$$

Likewise, if no electron energy is emitted by the wall, then the total heat current directed inward at the wall must be zero. This condition is expressed mathematically by the equation

$$H_-(R)=2\pi\int_0^{-1}\int_0^{\infty}(mv^2/2e)\times\mu v[f_0(R,v)+\mu f_{1r}(R,v)]v^2dv\ d\mu=0. \qquad (19)$$

When f_0 is Maxwellian, for example, then these conditions become

$$\Gamma_-(R)=\tfrac{1}{4}n(R)\overline{v}(R)-\tfrac{1}{2}\Gamma_r(R)=0$$

and

$$H_-(R)=\tfrac{1}{3}n(R)\overline{v}(R)u(R)-\tfrac{1}{2}H_r(R)=0,$$

respectively, where $\overline{v}(R)\equiv\sqrt{16eu(R)/3\pi m}$ is the mean speed. When f_0 is not Maxwellian, then the numerical factors $\frac{1}{4}$, $\frac{1}{3}$, and $16/3\pi$ are different.

D. Method of solution

The set of first-order ordinary differential equations (9)–(14) is solved by a Runge-Kutta technique, subject to the set of boundary conditions (15), (16), (18), and (19). Therefore, starting values for all six dependent variables must be selected to find a particular solution. Because boundary conditions (18) and (19) are specified at the wall where $r=R$, values of $u(0)$ and $(dH_r/dr)_{r=0}$ must be iterated to find the solution that satisfies them. The latter quantity is changed by iterating E_z. Therefore, the solution procedure can be summarized as follows: (i) Set initial values $\Gamma_r(0)=H_r(0)=E_r(0)=0$; (ii) guess values of $n(0)$, $u(0)$, and E_z; and (iii) solve Eqs. (9)–(14) out to $r=R$. If Eqs. (18) and (19) are not satisfied, then the procedure is repeated with new values of $u(0)$ and E_z. Finally, if discharge current I, defined by the equation

$$I=2\pi e\int_0^R[\mu(r)n(r)+\mu_i n_i(r)]E_z r\ dr,$$

is not equal to the desired value, then the entire process is repeated with a new value of $n(0)$. In the present work, relatively simple expressions for the transport coefficients μ, D, β, and G as functions of u are found from a 0D Boltzmann solution for the EEDF, as described below.

TABLE II. 0D Inelastic rates.

u (V)	$\tilde{\nu}_{gx}$ (cm^3/sec)	$\tilde{\nu}_{gi}$ (cm^3/sec)
6.0	4.0×10^{-14}	3.0×10^{-22}
7.0	5.0×10^{-12}	7.0×10^{-17}
8.0	4.5×10^{-11}	1.2×10^{-12}
9.0	1.3×10^{-10}	1.1×10^{-11}
10.0	2.6×10^{-10}	4.4×10^{-11}
11.0	4.5×10^{-10}	1.0×10^{-10}
12.0	7.3×10^{-10}	1.8×10^{-10}

E. Parametrization of transport coefficients

Transport coefficients and inelastic collision frequencies are parametrized by the average energy according to 0D Boltzmann calculations [23]. Because the total cross section for momentum transfer between electrons and neon atoms varies approximately as the 0.2 power of electron energy in the range 1–20 eV, the 0D Boltzmann transport coefficients can be represented approximately by the simple expressions $\mu N=1.48\times10^{23}u^{-0.7}$ V^{-1} cm^{-1} sec^{-1}, $DN=1.20\times10^{23}u^{0.3}$ cm^{-1} sec^{-1}, $\beta N=2.20\times10^{23}u^{0.3}$ cm^{-1} sec^{-1}, and $GN=1.34\times10^{23}u^{1.3}$ V cm^{-1} sec^{-1}, in this energy range. These values are obtained when the 0D f_0 is substituted in the recipes for transport coefficients given by Allis [19]. Similar expressions for neon transport coefficients with slightly different exponents of average energy are proposed in Ref. [21].

The corresponding inelastic collision frequencies are shown in Table II. The first six excited levels of atomic neon are lumped together to get excitation frequency $\tilde{\nu}_{gx}$. The density of the lumped excited state is treated in the same way as in Ref. [6]. The ionization cross section of the lumped excited state is assumed to be that of Vriens [11].

F. Results and discussion

1. Comparison with first-principles nonlocal kinetic method

To illustrate, the neon positive column described by Uhrlandt and Winkler [6] is simulated in the present work. Results corresponding to results shown in their Figs. 1, 4, 5a, and 5b are shown in Figs. 1, 2, 3, and 4, respectively. Figure 1 shows remarkably good agreement between the calculated space-charge potential $\phi(r)$ and the measured $\phi(r)$, which is assumed as input in Ref. [6]. Figure 2 shows a radial variation of the electron-ion density, average energy, radial particle current density, and radial heat current density. These curves are qualitatively similar to those of Uhrlandt and Winkler, but there are quantitative differences. For example, the inward radial heat current density H_r peaks at about 20×10^{15} V/cm^2/sec, whereas the peak value calculated by Uhrlandt and Winkler is about 9×10^{15} V/cm^2/sec. Figure 3 shows the radial variation of the ionization source, which includes stepwise as well as direct ionization. The total ionization source on axis is about 9

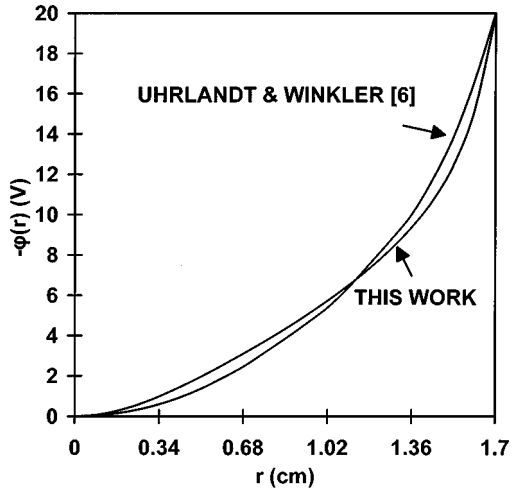

FIG. 1. Radial space-charge potential $-\phi(r)$. The upper curve is the measured potential assumed by Uhrlandt and Winkler, while the lower curve is the calculated output of the present work. The positive column conditions are 0.75-Torr neon, $I=10$ mA, and $R=1.7$ cm.

$\times 10^{14}$ cm^{-3} sec^{-1}, whereas Uhrlandt and Winkler found a value of about 4×10^{14} cm^{-3} sec^{-1}. Figure 4 shows the radial variation of the power output per unit volume $L(r)$, consisting of elastic and inelastic collision losses, and the power input per unit volume $P(r)$, consisting of Joule heating. Nonlocal behavior is evident in that these two quantities are not equal in each volume element of the discharge, even though their volume integrals are equal. As in previous comparisons, Fig. 4 shows different peak values of Joule heating and collision loss compared with those in Ref. [6]. The differences between all of these results and corresponding results of Ref. [6] can possibly be made smaller by using the same cross sections used in Ref. [6].

According to Eq. (7), the radial heat current density H_r is the sum of three components: $H_{\rm conv}$, $H_{\rm diff}$, and $H_{\rm cond}$. The

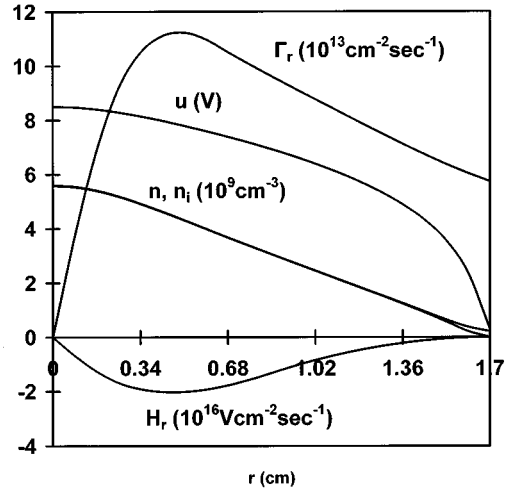

FIG. 2. Radial variation of the electron properties: electron density $n(r)$, average energy $u(r)$, radial current density Γ_r, and radial heat current density H_r. Compare with Fig. 4 of Ref. [6]. The positive column conditions are 0.75-Torr neon, $I=10$ mA, and $R=1.7$ cm.

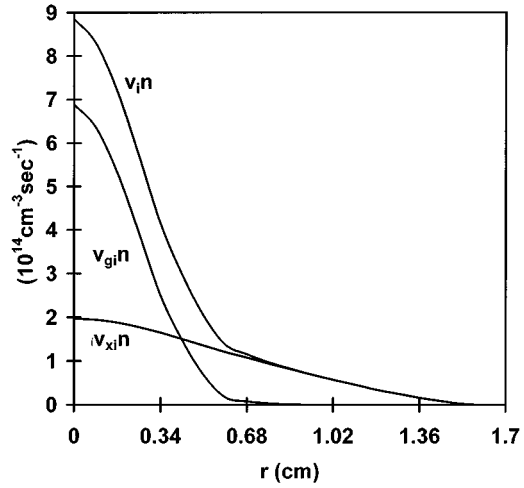

FIG. 3. Radial variation of the ionization rates: one step, $\nu_{gi}(r)n(r)$; two steps, $\nu_{xi}(r)n(r)$; total, $\nu_{gi}(r)n(r)+\nu_{xi}(r)n(r)$. ν_{xi} is based on the ionization from the 16.62-eV lumped state with the parabolic spatial distribution giving the average density equal to 10^{-5} times the ground-state density, similar to Ref. [6], and with the ionization cross section recommended by Vriens in Ref. [11]. Compare with Fig. 5a of Ref. [6]. The positive column conditions are 0.75-Torr neon, $I=10$ mA, and $R=1.7$ cm.

three components are defined as

$$H_{\rm conv}\equiv\frac{\beta}{\mu}\,\Gamma_r\,,$$

$$H_{\rm diff}\equiv\left(\frac{\beta}{\mu}-\frac{G}{D}\right)D\,\frac{dn}{dr}, \tag{20}$$

$$H_{\rm cond}\equiv -n\left(\frac{\partial G}{\partial u}-\frac{\beta}{\mu}\,\frac{\partial D}{\partial u}\right)\frac{du}{dr}.$$

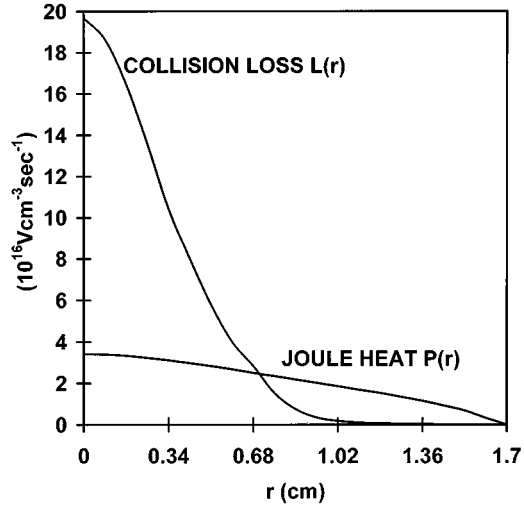

FIG. 4. Radial variation of the power input due to Joule heating and the power output due to collisional losses for the nonlocal moment method. Compare with Fig. 5b of Ref. [6]. The positive column conditions are 0.75-Torr neon, $I=10$ mA, and $R=1.7$ cm.

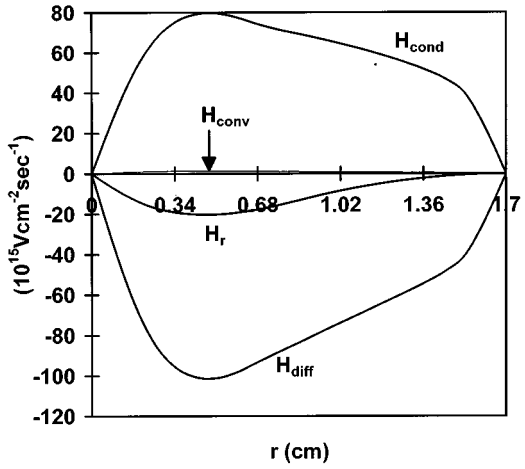

FIG. 5. Radial variation of the individual components of heat flow. The net heat flow H_r is equal to the sum $H_{\rm conv}+H_{\rm cond}+H_{\rm diff}$. The magnitude of the convective contribution to heat flow is on the order of 1% of the conductive and diffusive contributions. The positive column conditions are 0.75-Torr neon, $I=10$ mA, and $R=1.7$ cm.

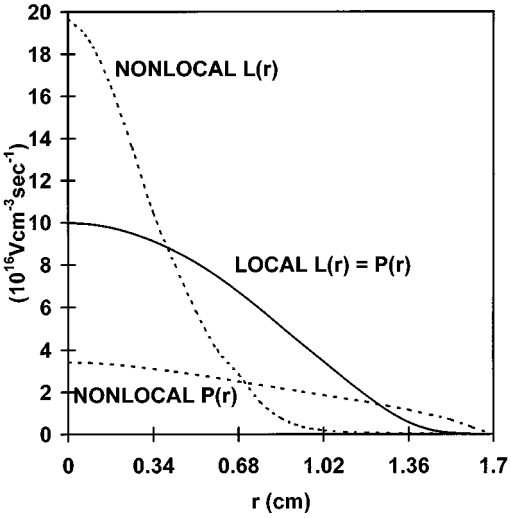

FIG. 6. Radial variation of the power input due to Joule heating and the power output due to collisional losses for the local moment method. Dashed curves are the same as in Fig. 4. The positive column conditions are 0.75-Torr neon, $I=10$ mA, and $R=1.7$ cm.

Figure 5 shows the three components of H_r plotted versus r. Note that the convective component is small compared to the other two components, which nearly cancel each other. Identification of radial heat flow as being composed of three components is not done in Ref. [6], so a comparison of these quantities cannot be made here.

Generally speaking, good qualitative agreement between results of the nonlocal moment method presented here and the results of the first-principles nonlocal kinetic method of Uhrlandt and Winkler is demonstrated. Proof is given in Table III, in which a comparison of measurable quantities is made for the four methods listed in Sec. I B: method 1, the first-principles nonlocal kinetic method; method 2, the nonlocal kinetic approximation method; method 3, the local moment method; and method 4, the nonlocal moment method. Entries in the second row of Table III are the results of Bailey and Bennett [24]. Entries in the third row of Table III are obtained by solving the local moment model constructed from the nonlocal moment model by setting $du/dr=0$ in Eq. (10), solving the resulting equation for H_r, substituting this H_r in Eq. (9) to give the familiar equation

$$\frac{dn}{dr}=-\frac{1}{D}\,\Gamma_r-\frac{\mu}{D}\,nE_r, \tag{21}$$

and solving this equation simultaneously with Eqs. (11), (12), and (14) while assuming radially invariant transport coefficients and collision frequencies. This table shows that calculated measurable quantities from the nonlocal moment method agree fairly well with those of the nonlocal kinetic method, while those of the other two methods do not agree as well. In particular, the axial electric field is almost twice as large for the local moment method and the wall potential is about three times larger as a consequence of average energy $u=8.2$ V being constant across the positive column. As mentioned above, it is possible that closer agreement between results of Uhrlandt and Winkler's 1D Boltzmann solution and those of the present nonlocal moment solution can be obtained by using the same cross sections they use.

The collision loss $L(r)$ and Joule heat $P(r)$, which are equal for the local moment method, are compared with those for the nonlocal moment method in Fig. 6. The half-width of the local moment $L(r)$ is significantly larger than that of the nonlocal moment $L(r)$ because $u=8.2$ V is constant across the positive column in the local moment calculation, whereas u varies radially in the nonlocal moment calculation as shown in Fig. 2.

2. Other comparisons

In the preceding subsection, the nonlocal moment method presented in this article is shown to be in good qualitative

TABLE III. Comparison of calculated measurable quantities. E_z and $\phi(r)$ are inputs to the 1D Boltzmann solution, but are calculated outputs in other methods; $\overline{n}=(2/R^2)\int n(r)r\,dr$; $-\phi_w$ is the wall potential measured relative to the positive column axis; J_w is the ion current density measured at wall; $PR=1.3$ Torr cm.

Method	$n(0)$ ($\rm cm^{-3}$)	$\overline{n}$ ($\rm cm^{-3}$)	$u(0)$ (V)	$L(0)$ ($\rm V\,cm^{-3}\,sec^{-1}$)	E_z (V/cm)	ϕ_w (V)	J_w ($\mu\rm A/cm^2$)	Source
1	5.8×10^9	2.7×10^9	7.4	1.0×10^{17}	2.17	20.0	9.1	[6]
2	4.5×10^9	1.9×10^9	7.5	1.2×10^{17}	2.53	22.1	7.2	[24]
3	4.4×10^9	1.3×10^9	8.2	1.0×10^{17}	4.25	58.9	14.6	present
4	5.6×10^9	2.0×10^9	8.5	2.0×10^{17}	2.24	19.9	9.2	present

agreement with the first-principles nonlocal kinetic method. Similarities between the nonlocal moment method formulation and that of other approximate methods have already been cited [18,20,21]. The procedure of parameterizing transport coefficients and collision frequencies by the average energy instead of by E_z/N in order to apply moment equations to nonequilibrium problems in gaseous electronics is widely used. An early example applying this procedure to a case of spatial nonequilibrium is [21]. Subsequent examples include studies of spatial nonequilibrium in the cathode fall [20], temporal nonequilibrium in pulsed fluorescent lamps [25], nonequilibrium motion in time-of-flight experiments [26], and spatial nonequilibrium near absorbing boundaries [18,27]. In [21], spatial nonequilibrium in a neon positive column with $PR=1.4$ Torr cm is studied with a formulation that includes moment equations similar to Eqs. (9) and (10) and simplifying assumptions of charge neutrality $n=n_i$ and $f_0(\epsilon)\propto\exp[-(\epsilon/\theta)^2]$. It is suggested in [21] that sometimes a good approximation is obtained by setting both Γ_r and H_r given by Eqs. (1) and (3), respectively, equal to zero and then eliminating E_r from the resulting equations to get

$$\frac{1}{\beta}\frac{d(Gn)}{dr}=\frac{1}{\mu}\frac{d(Dn)}{dr}.$$

This can be a useful approximation when the momentum-transfer collision frequency $\nu_m(\epsilon)$ is expressible as $\nu_m(\epsilon)\propto\epsilon^{(l+1)/2}$ because transport coefficients μ, D, β, and G are then proportional to u^j, where $j=-(l+1)/2$, $(1-l)/2$, $(1-l)/2$, and $(3-l)/2$, respectively, allowing analytic integration of the equation above to give $u/u_0=(n/n_0)^{\delta}$, where the constant δ is given by

$$\delta=D\left(\frac{\beta}{\mu}-\frac{G}{D}\right)\left[u\left(\frac{\partial G}{\partial u}-\frac{\beta}{\mu}\frac{\partial D}{\partial u}\right)\right]^{-1}.$$

The 0D transport coefficients given above in Sec. II E correspond to $l=0.4$ and $\delta=0.4$. The relation $u/u_0=(n/n_0)^{0.4}$ is satisfied approximately by the nonlocal moment method solutions for $n(r)$ and $u(r)$ shown in Fig. 2, even though the approximation $H_r=0$ is not satisfied as well as the approximation $\Gamma_r=0$, as pointed out in Ref. [6]. In contrast, $\delta=-2$ when $l=-\frac{3}{2}$, consistent with the conclusion reached in Sec. II F 3 namely, that u increases with increasing r when $l<-1$.

In addition to these similarities, there are some interesting differences. For example, it was found in [28] that average energy $u(r)$ increases with increasing r in He/Hg and Ar/Hg plasmas with $PR\approx1$ Torr cm. This result implies that the second derivative of u with respect to r is greater than 0 on axis. However, Eq. (10) predicts the opposite for all plasmas with a momentum-transfer collision frequency $\nu_m(\epsilon)$ that increases with increasing electron energy ϵ in the energy range of interest, which category includes He/Hg and Ar/Hg mixtures. By differentiating Eq. (10) with respect to r and evaluating the result at $r=0$, the following expression is found:

$$\left[\frac{d^2u}{dr^2}\right]_{r=0}=\left[D\frac{\partial}{\partial u}\left(\frac{G}{D}\right)\right]_{r=0}^{-1}\left[\frac{G}{Dn}\frac{d\Gamma_r}{dr}-\frac{1}{n}\frac{dH_r}{dr}-\left(\frac{\beta}{\mu}-\frac{G}{D}\right)\mu\frac{dE_r}{dr}\right]_{r=0}.$$

When the first derivatives appearing in this expression are eliminated by means of Eqs. (12)–(14) and (16) and when $\nu_i/\nu_{im}\ll1$, then this equation becomes

$$\left[\frac{d^2u}{dr^2}\right]_{r=0}=\frac{1}{2}\left[D\frac{\partial}{\partial u}\left(\frac{G}{D}\right)\right]_{r=0}^{-1}\left\{2\frac{m}{M}\nu_u u+\nu_x V_x+\nu_i\left[V_i+\frac{G}{D}-\left(\frac{\beta}{\mu}-\frac{G}{D}\right)\frac{\mu n}{\mu_i n_i}\right]-\mu E_z^2\right\}_{r=0}.$$

The right-hand side of this equation is dominated by the term proportional to the ratio of electron and ion mobilities, μ/μ_i, which is on the order of 100 for He/Hg and 1000 for Ar/Hg. Therefore, the right-hand side is negative because $\beta/\mu-G/D>0$ for both gas mixtures. The reader is reminded that the expression for $u''(0)$ given above is exact when the exact expression for $f_0(r,\epsilon)$, like the one obtained in Ref. [6], for example, is used to calculate transport coefficients. It is possible that the result found in [28] is due to the approximate way in which radial effects are included in the Boltzmann equation.

3. Mechanism causing radial nonequilibrium

The prevalent speculation about the mechanism responsible for radial nonequilibrium resulting in excess ionization on axis in low PR plasmas focuses on the qualitative argument that the radial space-charge field accelerates inward-bound electrons sufficiently to cause higher rates of inelastic collisions than encountered in radially uniform plasmas at the same value of E_z/N. If this speculative mechanism is the correct one, then it should occur when f_0 is Maxwellian [$\nu_m(\epsilon)$ independent of ϵ] or sub-Maxwellian [$\nu_m(\epsilon)$ decreasing with increasing ϵ] as well as when it is super-Maxwellian [$\nu_m(\epsilon)$ increasing with increasing ϵ]. However, the average energy is radially invariant, or nearly so, when f_0 is Maxwellian and increases with increasing r when f_0 is sub-Maxwellian, according to the analysis of Bernstein and Holstein [4]. Therefore, it appears that the speculation is incorrect. Instead, the mechanism responsible for excess ionization on axis in a low PR plasma with super-Maxwellian f_0 appears to be the inward-bound heat diffusion current density $H_{\rm diff}$, defined in Eq. (20), which carries heat from the outer region of the positive column where Joule heat $P(r)$ is larger than the collision loss $L(r)$ to the inner region where $P(r)<L(r)$, thus augmenting the Joule heat generated on axis by the external field. When f_0 is sub-Maxwellian, then $H_{\rm diff}>0$, the average energy increases with increasing r, and there is an ionization deficit on axis, in contradiction to the speculative mechanism mentioned above.

The direction of $H_{\rm diff}$ depends on the quantity $\beta/\mu-G/D$. For a momentum-transfer collision frequency $\nu_m(\epsilon)$ independent of electron energy ϵ (Maxwellian f_0), this quantity is zero. For $\nu_m(\epsilon)$ increasing with increasing ϵ, this

quantity is positive, causing inward heat diffusion and a negative gradient in the average energy. For $\nu_m(\epsilon)$ decreasing with increasing ϵ, it is negative, causing outward heat diffusion and a positive gradient in the average energy. Each coefficient in this expression is determined primarily by the behavior of bulk electrons, not that of tail electrons. Inward heat flow, for example, causes additional heating over and above Joule heating, increasing the average energy in the central region of the positive column over and above the corresponding equilibrium value. The shape of f_0 changes accordingly; there are fewer bulk electrons and more tail electrons, causing excess ionization over and above the corresponding equilibrium value [29]. It does not take much additional heating to give significantly more ionization. In the nonequilibrium neon positive column discussed at the beginning of this section, E_z/N is 8.4 Td and $u(0)=8.5$ V, whereas $u=7.4$ V in equilibrium at $E/N=8.4$ Td. The corresponding difference in the one-step ionization frequency is a factor of about 350 and the difference in excitation frequency is a factor of about 5 for these two values of average energy. Of course, this argument is qualitative because it is based on the 0D Boltzmann solution for f_0. However, the same general result can be expected when the exact f_0 of [6] is used to calculate transport coefficients and collision frequencies.

III. TRANSITION FROM NONEQUILIBRIUM TO EQUILIBRIUM AS *PR* INCREASES

The objective of this section is to derive a criterion that defines a range of pressure for which it can be assumed that average energy u is radially invariant, i.e., a range of pressure for which the local moment method, or local model, can be applied. This means that the power expended in collisions must be equal to the power generated by the external field *in each volume element of the discharge*. The approach taken to reach this objective is to assume that u is constant and then to derive a parametric relationship from the energy balance (13), which must be obeyed if this assumption is to be valid.

When u is constant Eq. (7) becomes

$$H_r=\frac{\beta}{\mu}\,\Gamma_r+\left(\frac{\beta}{\mu}-\frac{G}{D}\right)D\,\frac{dn}{dr},$$

whence

$$\frac{1}{r}\,\frac{d(rH_r)}{dr}=\frac{\beta}{\mu}\,\nu_i n+\left(\frac{\beta}{\mu}-\frac{G}{D}\right)\,\frac{D}{r}\,\frac{d}{dr}\,r\,\frac{dn}{dr}. \qquad (22)$$

The first term on the right-hand side, $(\beta/\mu)\nu_i n$, represents the energy needed to speed up newly created electrons to the average energy of the electron gas, so it could conceivably be considered part of the total energy expended in collisions. The second term on the right-hand side is not so easy to interpret; it represents a flow of energy due to diffusion, which can be directed either inward or outward, depending on the relative magnitudes of β/μ and G/D. After elimination of H_r from Eq. (13) by means of Eq. (22), the energy balance equation reads

TABLE IV. Ratio (25).

u (V)	Ratio	PR (Torr cm)
1.6	0.033	95
1.7	0.081	60
1.8	0.190	39

$$\frac{\beta}{\mu}\,\nu_i n+\left(\frac{\beta}{\mu}-\frac{G}{D}\right)\,\frac{D}{r}\,\frac{d}{dr}\,r\,\frac{dn}{dr}=\mu n E_z^2-\left(2\,\frac{m}{M}\,\nu_u u+\nu_x V_x+\nu_i V_i\right)n. \qquad (23)$$

The essence of the local model, embodied in the assumption that average energy u is radially invariant, is the condition that the quantity on the left-hand side of Eq. (23) be small compared with either term on the right-hand side. Simplification is obtained by invoking the ambipolar limit, in which case Eq. (21), combined with the radial ion current density $\Gamma_r=\mu_i n E_r$ gives the well-known Schottky equation

$$\frac{1}{r}\,\frac{d}{dr}\,r\,\frac{dn}{dr}+\frac{\nu_i}{D_a}\,n=0, \qquad (24)$$

where D_a is the classical ambipolar diffusion coefficient. Upon elimination of the derivative term from Eq. (23) by means of Eq. (24), the following condition is derived:

$$\tilde{\nu}_i\left[\left(\frac{\beta}{\mu}-\frac{G}{D}\right)\,\frac{D}{D_a}-\frac{\beta}{\mu}\right]\left(2\,\frac{m}{M}\,\tilde{\nu}_u u+\tilde{\nu}_x V_x+\tilde{\nu}_i V_i\right)^{-1}\ll 1, \qquad (25)$$

where $\tilde{\nu}_j\equiv\nu_j/N$, with N being the gas density. Note that this ratio does not depend explicitly on the gas density; it depends primarily on the isotropic part of the EEDF, denoted by f_0. It can be assumed that the local model is valid whenever this inequality is satisfied. Note also from Eq. (23) that satisfaction of inequality (25) implies

$$\mu E_z^2=2\,\frac{m}{M}\,\nu_u u+\nu_x V_x+\nu_i V_i,$$

which, in turn, implies f_0 and its moments, such as the average energy u and characteristic energy u_k, are radially invariant, consistent with the definition of the *local* model.

When f_0 is Maxwellian, due to a high electron density, for example, the term proportional to $D/D_a=\mu/\mu_i$ on the left-hand side of Eq. (25) is identically zero because $\beta/\mu=G/D$. In this case, the ratio (25) is small for most laboratory discharge conditions, implying that the local model is valid whenever f_0 is Maxwellian.

When f_0 is not Maxwellian, then $\beta/\mu\neq G/D$ and ratio (25) is not small for conditions normally found in low-pressure dc positive columns due to the magnitude of the factor D/D_a in the numerator. This conclusion can be illustrated by consideration of a dc positive column discharge in neon similar to that discussed in Sec. II. The variation of ratio (25) with average energy is shown in Table IV for neon, along with corresponding values of PR.

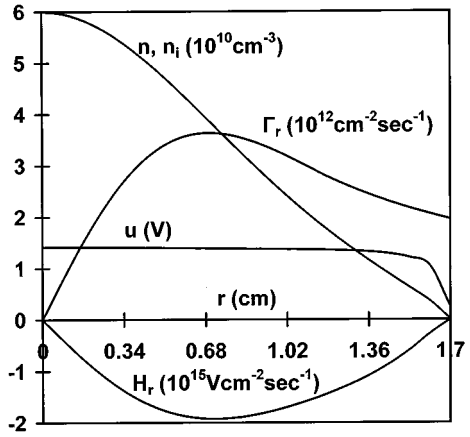

FIG. 7. Radial variation of the electron properties: electron density $n(r)$, average energy $u(r)$, radial current density Γ_r, and radial heat current density H_r. The positive column conditions are 50-Torr neon, $I=10$ mA, and $R=1.7$ cm. Note that some scales are different from those in Fig. 2.

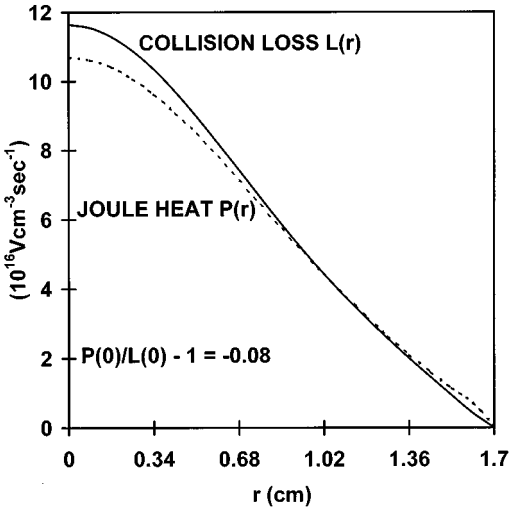

FIG. 8. Radial variation of the power input due to Joule heating and the power output due to collisional losses for the nonlocal moment method. The quantity $P(0)/L(0)-1$ is a measure of the departure from equilibrium. The positive column conditions are 50-Torr neon, $I=10$ mA, and $R=1.7$ cm.

According to this table, the average energy must be below 1.7 V for the local model to be valid. The value of PR at $u=1.7$ V is found as follows. The Schottky condition is

$$\nu_i=\frac{D_a}{\Lambda^2}=\frac{\mu_i u_k}{\Lambda^2},$$

where $\Lambda=R/2.4$ is the characteristic diffusion length for a cylinder of radius R. In terms of PR, this equation is

$$PR=\frac{2.4}{N_0}\left[\frac{\tilde{\mu}_i u_k}{\tilde{\nu}_i}\right]^{1/2}, \tag{26}$$

where $N_0=3.53\times10^{16}$ cm^{-3} is the gas density at 1 Torr pressure and $\tilde{\mu}_i\equiv\mu_i N=1.13\times10^{20}$ V^{-1} cm^{-1} sec^{-1} is the reduced mobility of Ne^+ in Ne [30]. At $u=1.7$ eV, the total ionization rate $\tilde{\nu}_{gi}+\tilde{\nu}_{xi}=2.1\times10^{-16}$ cm^3/sec and the value of u_k is 1.44 V. Substituting these values into the right-hand side of Eq. (26) gives $PR=60$ Torr cm. For comparison, Busch and Kortshagen [7] found from a numerical solution of the 1D Boltzmann equation that a gas density of 1×10^{18} cm^{-3}, equivalent to 28 Torr, is necessary to ensure that average energy in an argon positive column of 1 cm radius is radially invariant over most of the discharge cross section.

The qualitative discussion given above can be made more quantitative by solving Eqs. (9)–(14) at higher pressure. A pressure of 50 Torr is chosen for illustration. At this pressure, the electron density needed to give a current of 10 mA is an order of magnitude higher than at the pressure of 0.75 Torr discussed above. Therefore, it is reasonable to assume charge neutrality all the way to the wall, avoiding the necessity of solving Poisson's equation. In addition, ion inertia terms can be neglected, avoiding the necessity of solving the ion momentum balance equation. Instead, the relation $\Gamma_r=\mu_i n E_r$ can be used. These simplifications reduce the set of six ordinary differential equations to a set of four ordinary differential equations: Eqs. (9), (10), (12), and (13).

The solution of these equations for the macroscopic properties is shown in Fig. 7 for 50-Torr neon pressure. Note that the scales for the electron density and electron current density are different from those in Fig. 2. Note also that the electron heat current density peaks at a value that is about an order of magnitude lower than that in Fig. 2. Finally, note that the average energy is practically constant over most of the positive column cross section. The corresponding solutions for the collision loss $L(r)$ and Joule heating $P(r)$ are shown in Fig. 8. Note that they are almost equal at each radial position, indicating that the 50-Torr neon positive column can be described adequately by the local model. Note also that the value of the quantity $P(0)/L(0)-1$, which is a measure of departure from locality, is -0.08.

A comparison of measurable quantities for the local moment method and the nonlocal moment method at 50 Torr is shown in Table V. This table shows that poor agreement is obtained for wall potential ϕ_w even at 50 Torr, while there is little difference in other measurable quantities.

TABLE V. Comparison of calculated measurable quantities. $\overline{n}=(2/R^2)\int n(r)r\,dr$; $-\phi_w$ is the wall potential measured relative to the positive column axis; J_w is the ion current density measured at wall; $PR=85$ Torr cm.

Method	$n(0)$ (cm^{-3})	$\overline{n}$ (cm^{-3})	$u(0)$ (V)	$L(0)$ (V cm^{-3} sec^{-1})	E_z (V/cm)	ϕ_w (V)	J_w (μA/cm^2)
local moment	5.5×10^{10}	2.0×10^{10}	1.4	1.0×10^{17}	5.4	14.1	0.4
nonlocal moment	6.0×10^{10}	2.1×10^{10}	1.4	1.2×10^{17}	5.3	5.1	0.3

TABLE VI. PR (in units of Torr cm) range of validity.

Method	$PR<1$	$1<PR<10$	$10<PR<100$	$100<PR$
first-principles nonlocal kinetic	yes	yes	yes	yes
nonlocal kinetic approximation	yes	?	no	no
local moment	no	no	?	yes
nonlocal moment	yes	yes	yes	yes

A word of caution is necessary: At 50 Torr pressure, most of the collision loss is due to elastic collisions, so there may be some gas heating. The rise δT_g in gas temperature T_g in the case of 50 Torr can be estimated from the formula

$$\frac{\delta T_g}{T_g}=\frac{L(0)\Lambda^2}{\kappa T_g},$$

where $L(0)=1.2\times10^{17}$ V cm^{-3} sec^{-1}=19.2 mW/cm^3 is the collision loss on axis, $\Lambda=R/2.4$ is the characteristic diffusion length for a cylinder of radius R, and $\kappa=4.55\times10^{-4}$ W/cm/deg is the thermal conductivity of neon [31]. For $R=1.7$ cm and $T_g=273$ K, this equation gives $\delta T_g=21$ K. For higher pressure, $\delta T_g/T_g$ will be correspondingly higher if the current I is held fixed at 10 mA because $L(0)$ will be higher.

IV. SUMMARY

In this work a moment theory of electron transport in a strong electric field is applied to the stationary nonequilibrium positive column. The theory uses equations describing the conservation of electron density, momentum, and energy. The importance of the electron energy balance, which is frequently ignored in positive column analysis, is emphasized. The balance equations are derived by taking moments of the Boltzmann equation *after* the two-term Legendre expansion of the EEDF is made, a procedure that is not generally followed, but is necessary for consistency and accuracy when dealing with real gases.

Theoretical justification of the method is given in previous work [18], where two important features of the method are emphasized: (i) The method gives exact results for the momentum and energy of electrons under equilibrium conditions in a strong electric field, unlike theories that assume that the EEDF has a simple form, such as a Maxwellian, and (ii) the method provides an accurate description of electron flow when there are significant temporal and spatial departures from equilibrium, also unlike theories that assume that the EEDF has a simple form, such as a Maxwellian.

The moment equations of this method contain transport coefficients and collision frequencies that are parametrized by the average energy according to numerical solutions of the 0D Boltzmann equation for different values of E_z. Model results in the nonequilibrium regime agree closely with published results of a numerical solution of the 1D Boltzmann equation, including results for radial heat flow in the electron gas with radially varying average energy. It is shown that three separate processes account for radial heat flow: convection, conduction, and diffusion. In the example chosen for illustration of the method, the convection component is small, while the conduction and diffusion components are large and opposite in sign, nearly canceling each other.

The parametrization of transport coefficients and collision frequencies by the average energy instead of E_z is a key assumption of the method described in this paper. While this assumption ensures accuracy of the method for high values of PR where equilibrium conditions prevail, accuracy at low values of PR where nonequilibrium conditions prevail can be questioned. It is the opinion of this author, however, that the accuracy of the method for low values of PR is very good provided that 0D transport coefficients and collision frequencies are expressible as single-valued functions of average energy.

V. CONCLUSIONS

It is concluded from this work that positive column behavior at any pressure can be described adequately by moment equations when radial heat flow in the electron gas is taken into account and when electron transport coefficients and relevant collision frequencies are assumed to be related to the radially varying average energy according to 0D Boltzmann calculations. It is also concluded that the formulation presented here predicts a pressure boundary above which the local model is valid. For the neon positive column with 1.7 cm radius studied in this paper, this pressure boundary is estimated to be in the neighborhood of 35 Torr, or $PR=60$ Torr cm. The solution of the nonlocal moment formulation at a pressure of 50 Torr, where $PR=85$ Torr cm, supports this estimate, showing that average energy is constant within 7% over the central 80% of the positive column.

The PR range of validity of the four theoretical methods discussed in this article is given in Table VI. The limits of the four ranges of PR are arbitrary. The question marks mean that the method can be used in this particular range of PR, but it must be recognized that results are inaccurate to some degree or another. For $PR>100$, the radial variation in gas temperature should be taken into account.

ACKNOWLEDGMENTS

Special thanks are due Lev Tsendin for leading the author step by step through the derivation of the second term in the expansion of $f_0(r,\epsilon)=f_{00}(\epsilon)+f_{01}(r,\epsilon)+\cdots$, which is the basis of the nonlocal kinetic approximation, which he has investigated so thoroughly. Special thanks go also to Art Phelps for suggesting the problem of establishing the pressure boundary between local and nonlocal models. In addition, the author wishes to acknowledge the assistance of the following people: W. F. Bailey and E. J. Bennett for provid-

ing the numerical solution of the nonlocal kinetic approximation method for neon with $PR = 1.3$ Torr cm and 0D Boltzmann calculations of neon transport coefficients, Art Phelps and Tim Sommerer for reviewing the manuscript, and Ed Richley for numerous discussions on the local model versus the nonlocal model. Last, but certainly not least, the author would like to thank Vladimir Kolobov for focusing the author's attention on the nonlocal model.

[1] M. J. Druyvesteyn and F. M. Penning, Rev. Mod. Phys. **12**, 87 (1940).
[2] G. Francis, in *The Glow Discharge at Low Pressure*, edited by S. Flugge, Handbuch der Physik Vol. 22 (Springer, Berlin, 1956), p. 53.
[3] J. L. Blank, Phys. Fluids **11**, 1686 (1968).
[4] I. B. Bernstein and T. Holstein, Phys. Rev. **94**, 1475 (1954).
[5] L. D. Tsendin, Zh. Eksp. Teor. Fiz. **66**, 1638 (1974) [Sov. Phys. JETP **39**, 805 (1974)]; Zh. Tekh. Fiz. **47**, 1839 (1977) [Sov. Phys. Tech. Phys. **22**, 1066 (1977)]; **48**, 1569 (1978) [**23**, 890 (1978)]; Plasma Sources Sci. Technol. **4**, 200 (1995).
[6] D. Uhrlandt and R. Winkler, J. Phys. D **29**, 115 (1996).
[7] C. Busch and U. Kortshagen, Phys. Rev. E **51**, 280 (1995).
[8] W. Schottky, Z. Phys. **25**, 635 (1924).
[9] L. Tonks and I. Langmuir, Phys. Rev. **34**, 876 (1929).
[10] L. G. H. Huxley and R. W. Crompton, *The Diffusion and Drift of Electrons in Gases* (Wiley, New York, 1974).
[11] L. Vriens, J. Appl. Phys. **44**, 3980 (1973).
[12] R. Lagushenko and J. Maya, J. Illum. Eng. Soc. **14**, 306 (1984).
[13] J. H. Ingold, Bull. Am. Phys. Soc. **41**, 1345 (1996).
[14] G. J. Parker, W. N. G. Hitchon, and J. E. Lawler, Phys. Rev. E **50**, 3210 (1994).
[15] J. E. Lawler, U. Kortshagen, and G. J. Parker, Bull. Am. Phys. Soc. **41**, 1345 (1996).
[16] U. Kortshagen, J. E. Lawler, and G. J. Parker, Bull. Am. Phys. Soc. **41**, 1345 (1996).
[17] G. J. Parker, U. Kortshagen, and J. E. Lawler, Bull. Am. Phys. Soc. **41**, 1345 (1996).
[18] A thorough theoretical justification of this key assumption is given by G. Roumeliotis and L. E. Cram, J. Phys. D **22**, 113 (1989); application to temporal nonequilibrium caused by rapidly varying $E_z(t)$ is also given. See also L. E. Cram, Phys. Rev. A **43**, 4480 (1991) for application to spatial nonequilibrium near absorbing boundaries.
[19] See *Electrons, Ions, and Waves: Selected Works of William Phelps Allis*, edited by S. C. Brown (MIT Press, Cambridge, MA, 1967), p. 169.
[20] A similar approach is taken by I. Abbas and P. Bayle, J. Phys. D **14**, 649 (1981), to study *nonequilibrium* motion of electrons in the cathode fall.
[21] D. Herrmann, A. Rutscher, and S. Pfau, Beit. Plasmaphys. **11**, 75 (1971). It is noted by these authors that assumption of a Maxwellian f_0 results in radially invariant average energy, approximately, while assumption of a non-Maxwellian f_0 results in radially varying average energy, as noted here.
[22] A similar derivation was given by W. P. Allis and D. J. Rose in their now classic paper on the transition from free diffusion to ambipolar diffusion, Phys. Rev. **93**, 84 (1954).
[23] W. F. Bailey and E. J. Bennett (private communication). Using ELENDIF, a 0D Boltzmann code marketed by Kinema Software, P.O. Box 1147, Monument, CO 80132, Bailey and Bennett provided the author with a 0D Boltzmann computation of μ, D, β, G, and collision frequencies versus average energy for neon. The 0D Boltzmann code ELENDIF is described by W. L. Morgan and B. M. Penetrante, Comput. Phys. Commun. **58**, 127 (1990).
[24] W. F. Bailey and E. J. Bennett (private communication); see also Bull. Am. Phys. Soc. **41**, 1344 (1996).
[25] M. E. Duffy and J. H. Ingold, Bull. Am. Phys. Soc. **34**, 307 (1989).
[26] J. H. Ingold, Phys. Rev. A **42**, 950 (1990).
[27] J. H. Ingold, Phys. Rev. A **43**, 3086 (1991).
[28] M. J. Hartig and M. J. Kushner, J. Appl. Phys. **73**, 1080 (1992).
[29] S. Pfau, J. Rohman, D. Urhlandt, and R. Winkler, Contrib. Plasma Phys. **36**, 449 (1996). Compare curves for the 1D f_0/n_e on axis and the 0D F_0 on axis in Fig. 6 of this reference.
[30] E. W. McDaniel, *Collision Phenomena in Ionized Gases* (Wiley, New York, 1964), p. 466, Table 9-9-1.
[31] S. Chapman and T. G. Cowling, *The Mathematical Theory of Non-Uniform Gases* (Cambridge University Press, Cambridge, England, 1960), Chap. 13, p. 241, Table 22.